THE JOURNAL OF BIOLOGICAL CHEMISTRY VOL. 292, NO. 4, pp. 1414–1425, January 27, 2017
© 2017 by The American Society for Biochemistry and Molecular Biology, Inc. Published in the U.S.A.

Metnase Mediates Loading of Exonuclease 1 onto Single Strand Overhang DNA for End Resection at Stalled Replication Forks*

Received for publication, June 27, 2016, and in revised form, December 13, 2016 Published, JBC Papers in Press, December 14, 2016, DOI 10.1074/jbc.M116.745646

Hyun-Suk Kim[‡], Elizabeth A. Williamson[§], Jac A. Nickoloff[¶], Robert A. Hromas[§], and Suk-Hee Lee[‡1]

From the [‡]Department of Biochemistry and Molecular Biology, Indiana University School of Medicine, Indianapolis, Indiana 46202, the [§]Department of Medicine, University of Florida and Shands Health Care System, Gainesville, Florida 32610, and the [¶]Department of Environmental and Radiological Health Sciences, Colorado State University, Fort Collins, Colorado 80523

Edited by Patrick Sung

Stalling at DNA replication forks generates stretches of single-stranded (ss) DNA on both strands that are exposed to nucleolytic degradation, potentially compromising genome stability. One enzyme crucial for DNA replication fork repair and restart of stalled forks in human is Metnase (also known as SETMAR), a chimeric fusion protein consisting of a su(var)3–9, enhancer-of-zeste and trithorax (SET) histone methylase and transposase nuclease domain. We previously showed that Metnase possesses a unique fork cleavage activity necessary for its function in replication restart and that its SET domain is essential for recovery from hydroxyurea-induced DNA damage. However, its exact role in replication restart is unclear. In this study, we show that Metnase associates with exonuclease 1 (Exo1), a 5′-exonuclease crucial for 5′-end resection to mediate DNA processing at stalled forks. Metnase DNA cleavage activity was not required for Exo1 5′-exonuclease activity on the lagging strand daughter DNA, but its DNA binding activity mediated loading of Exo1 onto ssDNA overhangs. Metnase-induced enhancement of Exo1-mediated DNA strand resection required the presence of these overhangs but did not require Metnase's DNA cleavage activity. These results suggest that Metnase enhances Exo1-mediated exonuclease activity on the lagging strand DNA by facilitating Exo1 loading onto a single strand gap at the stalled replication fork.

DNA-damaging agents as well as inhibitors of deoxyribonucleotide synthesis and DNA polymerase action block the progression of replication forks (1, 2). Replication fork stalling induces uncoupling between DNA polymerases and the replicative DNA helicases and generates stretches of ssDNA[2] on both strands that are exposed to nuclease attack (1–7). Replication fork repair and restart in eukaryotes are complex and poorly understood (1, 5, 7, 8). Upon replication fork arrest from deoxyribonucleotide depletion after hydroxyurea (HU) treatment, uncoupling of DNA polymerases and helicase generates ssDNA overhangs on both leading and lagging strands. Restart of stalled replication forks can occur via the reannealing of ssDNA, or forks can undergo regression and pairing of the newly synthesized strands to form a Holliday junction structure ("chicken foot"). When free 5′-ends are present, end resection creates 3′-ssDNA on which Rad51 can load, and Rad51-mediated DNA displacement loop formation eventually allows reloading of the replication machinery for fork restart. Rad51-mediated homologous recombination (HR) also mediates fork reversal for restart of replication (9, 10). Holliday junctions can also be processed into a one-ended double strand break (DSB), and fork restart is then achieved through Rad51-mediated homologous recombination repair (1, 5, 7, 8). Although homologous recombination repair is a preferred pathway in restart of stalled replication forks (1, 5, 8, 11, 12), the detailed mechanism(s) and the factors involved are not well understood.

Stalled replication forks often require the generation of an intrinsic DSB to begin the 5′-end resection that initiates recombination-mediated fork repair (1, 7, 8, 13, 14). The stressed fork can do this in at least two ways: the fork can reverse into a chicken foot structure with a one-sided DSB, or a nuclease can generate a DSB at the stalled fork as part of the restart process. If a stalled fork is not repaired, it can collapse into a variety of structures that make restart difficult (8, 15–17) and can result in genomic instability, leading to cell death or neoplastic transformation (2, 8, 11). Repair pathway choice at stalled forks is important for genomic stability because unopposed classical non-homologous end joining (cNHEJ), such as seen in malignancies with inherited BRCA1 or BRCA2 deficiencies, results in fusion of the one-sided DNA ends at damaged replication forks (12, 18–22). These chromosomal fusions at stalled forks can cause severe genome instability, resulting in catastrophic mitoses with gross nuclear abnormalities, such as nuclear bridges and micronuclei (8, 12, 18, 21, 23). Preventing cNHEJ by

* This work was supported by National Institutes of Health Grants R01 CA151367 (to S.-H. L.), R01 GM084020 (to J. A. N. and R. A. H.), and R01 CA139429 (to R. A. H.) and by the Indiana University Simon Cancer Center. The authors declare that they have no conflicts of interest with the contents of this article. The content is solely the responsibility of the authors and does not necessarily represent the official views of the National Institutes of Health.

[1] To whom correspondence should be addressed: Dept. of Biochemistry and Molecular Biology, Indiana University Simon Cancer Center, Indiana University School of Medicine, Indianapolis, IN 46202. Tel.: 317-278-3464; Fax: 317-274-8046; E-mail: slee@iu.edu.

[2] The abbreviations used are: ss, single-stranded; Exo1, exonuclease 1; HU, hydroxyurea; HR, homologous recombination; DSB, double strand break; cNHEJ, classical non-homologous end joining; alt-EJ, alternative end joining; BLM, Bloom syndrome protein; IR, ionizing radiation; HTH, helix-turn-helix; SET, su(var)3–9, enhancer-of-zeste and trithorax; CtIP, CtBP (C-terminal binding protein) interacting protein.

repressing 53BP1 rescues these nuclear defects (19). Thus, HR is the preferred repair pathway for stalled replication forks to prevent genomic instability (1, 5, 8, 11, 12). There is accumulating evidence that DSB pathway choice between cNHEJ and HR is mediated by 5′-end resection (13, 14, 24). End resection for HR is likely a two-step process where CtIP and Mre11 nucleolytically resect short 5′-tracks with Dna2 and especially Exo1 resecting longer tracks (13, 14, 17, 25, 26), generating long 3′-ss-tracts. The choice between different DSB repair pathways is tightly regulated, and DNA end resection represents a primary regulatory step (27). The ssDNA tails created at DSBs also play a critical role in DNA damage (checkpoint) response (27, 28). DNA resection decreases cNHEJ efficiency (27) but is essential for the homology-mediated DSB repair pathways, alternative end joining (alt-EJ), and HR (17, 29–31). The balance between cNHEJ, alt-EJ, and HR is controlled by key DNA end resection factors (27). Alt-EJ and HR share the initial end resection step of a limited resection at DSB sites by Mre11/CtIP (17, 22, 25, 31–35), which is necessary for subsequent recruitment of Exo1 along with Bloom syndrome protein (BLM) and its paralog Werner syndrome ATP-dependent helicase (WRN) to mediate extensive end resection (22, 25, 34, 36–38). However, alt-EJ in contrast to HR does not seem to require γ-H2AX (17), suggesting that the initial end resection event in the alt-EJ pathway is distinct from the HR repair pathway.

Metnase is a SET-transposase domain chimeric protein with endonuclease activity that plays a crucial role in restart of stalled replication forks (39–41). In this study, we found that Metnase associates with Exo1 and is involved in DNA processing at the stalled replication fork. Metnase not only mediates loading of Exo1 onto single strand overhangs but also enhances Exo1-mediated resection, suggesting that Metnase enhances Exo1's 5′-exonuclease activity on the lagging daughter DNA by mediating Exo1 loading onto gapped DNA.

Results

Metnase Interacts with Exo1 and Promotes DNA Processing at Stalled Forks—Metnase's SET domain and its DNA cleavage activity derived from the transposase domain are essential for Metnase's function in restart of stalled replication forks (40, 41) This suggests that Metnase has multiple roles in replication restart. In an effort to clarify these roles, we examined association of Metnase with DNA end-processing nucleases that function at stalled replication forks (25, 26, 34, 37, 42–44). Metnase expression was not affected by HU, but the Exo1 level was markedly reduced after HU treatment (Fig. 1*A*, *lane 1 versus lane 2*). This observation is in keeping with the previous finding by others that human Exo1 is phosphorylated and rapidly degraded through ubiquitin-proteosome pathways in response to HU treatment (45). We found that Metnase associates with Exo1 in the presence of DNase I treatment regardless of replication stress (Fig. 1*A*). A physical interaction was also observed between two purified proteins (Fig. 1*B*), indicating that there is a direct interaction between Metnase and Exo1. To further analyze the Metnase-Exo1 interaction, we examined deletion mutants of Metnase and Exo1 for physical interaction. A mutant Metnase lacking the C terminus (ΔTransposase) failed to interact with Exo1 (Fig. 1*C*), whereas a mutant Exo1 lacking the N terminus (Δ1–404) did not pull down Metnase in the co-immunoprecipitation experiment (Fig. 1*D*). These findings suggest that Metnase directly interacts with Exo1, and these two proteins may function together at replication forks.

We next examined whether Metnase affects DNA processing at stalled replication forks. For this, we measured HU-induced generation of ssDNA by immunostaining of newly incorporated BrdU when the cells were not treated with agents that denature DNA as described previously (34, 46). In this analysis, only BrdU present in ssDNA was detected. As shown in Fig. 2*A*, there were fewer BrdU foci in Metnase-repressed cells compared with control cells after HU treatment, suggesting that DNA end resection is attenuated when Metnase is repressed. We also saw a marked reduction in BrdU foci with Exo1 knockdown; a further reduction in BrdU foci was observed in Metnase- and Exo1-repressed cells (Fig. 2, *A* and *B*). To further assess Metnase involvement in the processing of stalled replication forks, cells transfected with scrambled siRNA or si-Metnase were labeled with IdU for 45 min prior to prolonged exposure to HU, and DNA resection on nascent DNA was analyzed by measuring lengths of IdU-labeled fibers (10) (Fig. 2*C*). Nascent IdU tracks were substantially longer in Metnase-depleted cells compared with control when replication forks were stalled, and IdU tracts were also shorter in Exo1- and doubly depleted cells (Fig. 2, *D* and *E*). After 10 h of HU treatment, the mean track lengths of control and Metnase-depleted cells were 5.9 and 9.3 μm, respectively ($p < 0.001$; Fig. 2*E*), suggesting that Metnase plays a crucial role in the processing of stalled replication forks. Metnase also promoted Exo1-mediated resection at DSB sites following ionizing radiation (IR) (Fig. 2*F*), indicating that Metnase's action would be more general and not limited to forks.

To see whether Metnase's involvement in DNA resection is linked to recombination repair at stalled forks, we examined fork restart and formation of Rad51 foci after HU treatment. Formation of replication protein A foci is also a common readout for ssDNA at stalled forks (41) but was not included here because they can be formed at replication forks without DNA resection (47, 48). Repression of Exo1 had very little impact on fork restart after a short (1-h) HU exposure (Fig. 2, *G* and *H*), whereas si-Metnase showed a marked delay after 1-h HU treatment (Fig. 2, *G* and *H*). In contrast, a marked reduction in formation of Rad51 foci was observed with Metnase- and Exo1-repressed cells compared with control cells after a long HU exposure (Fig. 2, *I* and *J*). Together, these results suggest that Exo1 is not a major player at stalled fork following a short HU exposure but may play a crucial role at collapsed forks that require recombination repair for fork restart. Metnase, in contrast, could be involved in preventing fork reversal in response to a short exposure to HU (9).

Metnase Enhances Exo1-mediated 5′-End Resection on Model Replication Fork Structures—Metnase possesses DNA endonuclease activity that cleaves replication fork structures at the ssDNA gap of the lagging strand (40). End resection nucleases, such as Exo1, Dna2, and CtIP, cleave these structures poorly because they require a free 5′-OH end to begin exonucleolysis (49–52). Metnase-mediated fork endonucleolytic cleavage not only generates a free 5′-OH end on the lagging

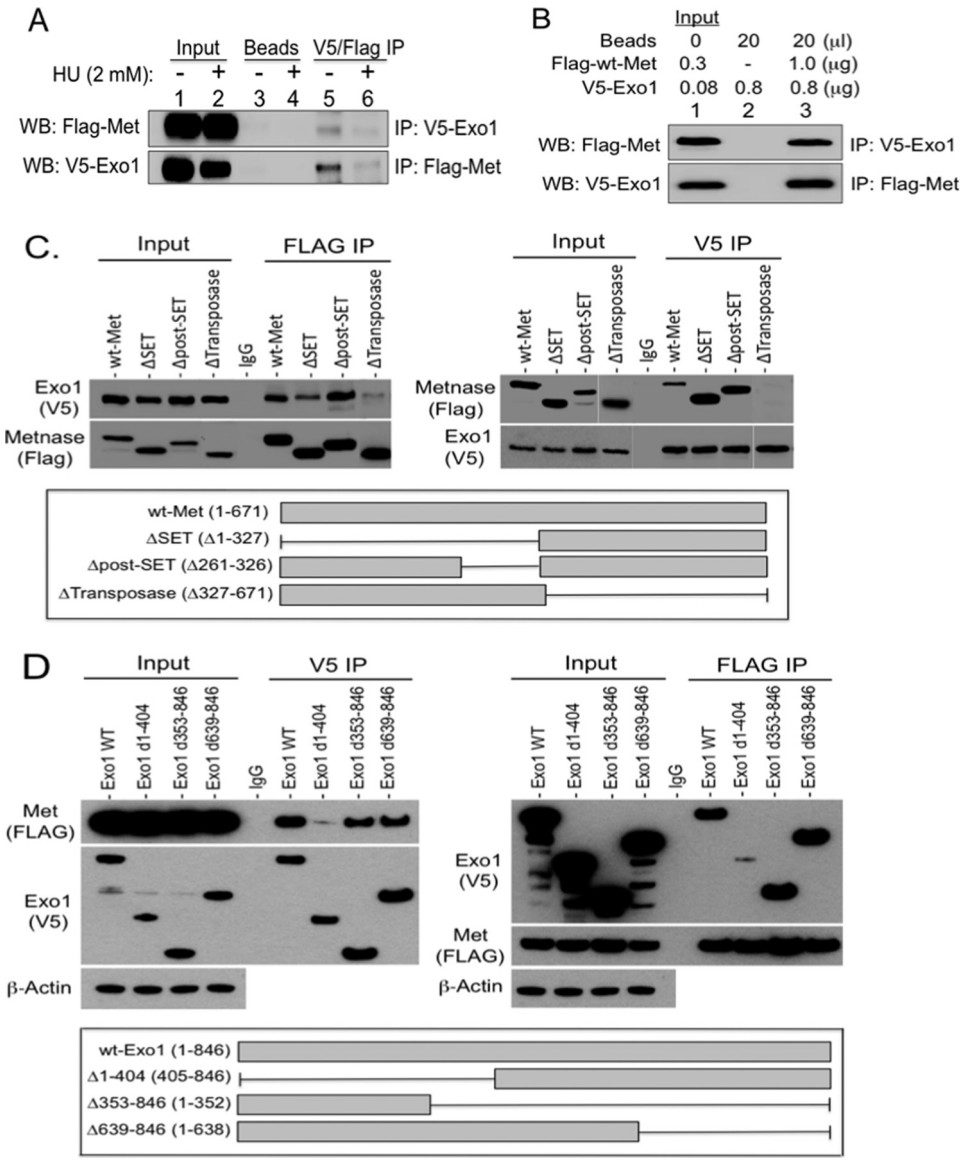

FIGURE 1. **Physical interaction of Metnase with Exo1.** *A*, reciprocal co-immunoprecipitation of FLAG-Metnase (*Met*) and V5-Exo1 in HEK293 cells. Cells stably expressing FLAG-Metnase were transiently transfected with a vector harboring V5-Exo1 for 30 h prior to 18-h HU treatment (0 or 2 mM). Lysates were pretreated with DNase I (4 units), incubated at 37 °C for 10 min, and immunoprecipitated (*IP*) using 1 mg of protein. Protein samples were incubated overnight at 4 °C, and 20 μl of protein G-agarose beads were added and incubated for 1 h at 4 °C. After removing supernatants, beads were washed four times and analyzed by Western blotting (*WB*). One-tenth of protein (0.1 mg) was used for input control. *B*, direct interaction of Metnase with Exo1. The indicated amounts of purified WT Metnase and/or purified Exo1 were incubated together for 10 min prior to co-immunoprecipitation and Western blotting using either a FLAG or V5 antibody. *C* and *D*, identification of Metnase (*C*) and Exo1 (*D*) domains that are crucial for the Metnase-Exo1 interaction. HEK293 cells stably expressing V5-Exo1 (*C*) or FLAG-Metnase (*D*) were transfected with full-length and truncated versions of FLAG-Metnase (*C*) or V5-Exo1 (*D*) and immunoprecipitated with FLAG or V5 antibody, and Western blots were probed with V5 or FLAG antibody. Schematic diagrams of WT Metnase/WT Exo1 and the deletion mutants are in the *bottom panels*.

parental DNA but also produces the 3′-ss-overhang for 5′-end resection of the daughter strand DNA (Fig. 3*B*) (40, 41), suggesting that Metnase may play a unique role in initiating 5′-end resection at stalled replication forks. To explore this further, we analyzed nucleolytic processing of model replication fork structures *in vitro* by WT Metnase and/or WT Exo1. Metnase displayed minor end cleavage activity that was unaffected by Exo1 (Fig. 3, *C*, *lanes 2* and *3 versus lanes 6* and *7*, and *D*). In contrast, Exo1's nuclease activity on the lagging nascent DNA was markedly enhanced in the presence of Metnase (Fig. 3, *C*, *lane 4 versus lanes 6* and *7*, and *D*). No DNA resection was observed with a nuclease-dead mutant of Exo1 activity (D173A) (37) even in the presence of WT Metnase (Fig. 3, *C* and *D*). Because Metnase's catalytic motif (DDN) was necessary to promote restart of stalled forks (40), we examined whether Metnase's DNA cleavage activity plays a role in Exo1-mediated resection of the lagging strand DNA. Exo1-mediated resection of the lagging daughter DNA was enhanced by both WT Metnase and the catalytically dead D483A mutant, (Fig. 3*E*), suggesting that Metnase enhances Exo1-mediated resection by a mechanism that is independent of lagging daughter strand cleavage. Although Metnase's DNA cleavage activity is not involved in Exo1-mediated resection of the lagging daughter DNA (Fig. 3, *E* and *F*), cells overexpressing a Metnase mutant lacking DNA cleavage activity (D483A) showed a marked reduction in generation of ssDNA as measured by formation of BrdU foci after

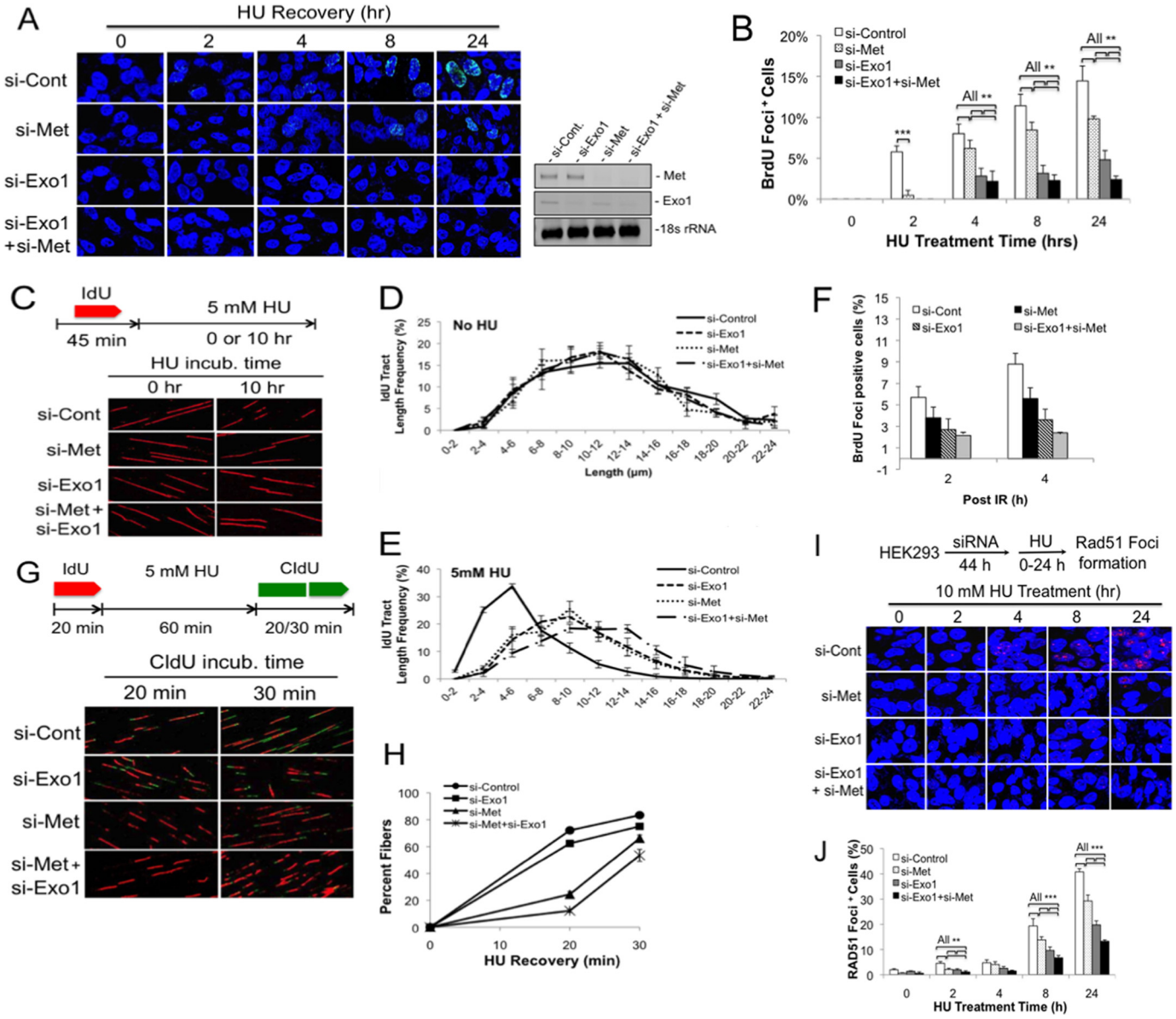

FIGURE 2. **Metnase and Exo1 are involved in stalled fork processing.** *A* and *B*, representative images (*A*) and quantitation (*B*) of stalled fork processing stained with anti-BrdU antibodies (*green*) without denaturation of genomic DNA in HEK293 cells with and without Metnase and/or Exo1 depletion after HU treatment. DAPI nuclear counterstain is *blue*. Plotted are means ± S.E. for three determinations with >100 images scored per determination. *Error bars* represent S.E. **, $p < 0.05$; ***, $p < 0.01$, *t* tests. *C*, schematic of DNA fiber track analysis (*top*) and representative DNA fiber images (*bottom*) of stalled fork processing. *D* and *E*, IdU track length distributions in control and Metnase- and/or Exo1-depleted cells after HU treatment. Data are from three independent experiments with >200 tracks scored per condition in each experiment. *Error bars* represent S.E. *F*, DNA resection of HEK293 cells transfected with si-control (*si-Cont*), si-Metnase (*si-Met*), si-Exo1, and si-Metnase + si-Exo1 after IR treatment. After incubation (*incub.*) with 40 μM BrdU for 36 h, cells were treated with IR (20 grays), harvested in 2 and 4 h, stained, and measured for BrdU foci-positive cells. *G* and *H*, Metnase, not Exo1, plays a role in fork restart after a short HU exposure. *Top*, dual labeling protocol for replication restart using DNA fiber analysis. *Bottom*, representative confocal microscope images (*G*) and quantitation (*H*) of replication tracks from HEK293 cells transfected with si-control (*top row*), si-Exo1 (*second row*), si-Metnase (*third row*), and si-Metnase + si-Exo1 (*bottom row*). Cells were treated with 5 mM HU for 1 h prior to pulse labeling with CldU for 20 and 30 min. *I* and *J*, representative images (*I*) and quantitation (*J*) of Rad51 foci (*red*) in HEK293 cells after replication stress (HU treatment) with and without Metnase and/or Exo1 depletion. DAPI nuclear counterstain is *blue*. Data represent average ± S.E. for three distinct determinations per condition. *Error bars* represent S.E. **, $p < 0.05$; ***, $p < 0.01$, *t* tests.

HU treatment (Fig. 3, *G* and *H*), suggesting that Metnase's DNA cleavage activity does play an important role in resection of stressed forks *in vivo*.

Metnase Mediates Loading of Exo1 onto Single Strand Overhang DNA—Because enhancement of Exo1-mediated resection by Metnase does not require its DNA cleavage activity (Fig. 3*E*), we reasoned that Metnase might be involved in loading Exo1 onto DNA. To test this, we performed a pulldown experiment in which WT Metnase was incubated with 3′-biotinylated DNA to assay protein-DNA binding by using streptavidin-agarose beads, and the protein-DNA interaction was analyzed by Western blotting. WT Metnase was effectively pulled down with single strand overhangs but not with blunt-ended dsDNA (Fig. 4*A*), suggesting that Metnase requires ss-overhang for binding to dsDNA. Exo1 alone showed little or no interaction with single strand overhangs (Fig. 4*B*, *top panel*, *lanes 2* and *3*), but the Exo1-DNA interaction was markedly enhanced in the presence of WT Metnase (Fig. 4*B*, *top panel*, *lanes 4* and *5*). A substitu-

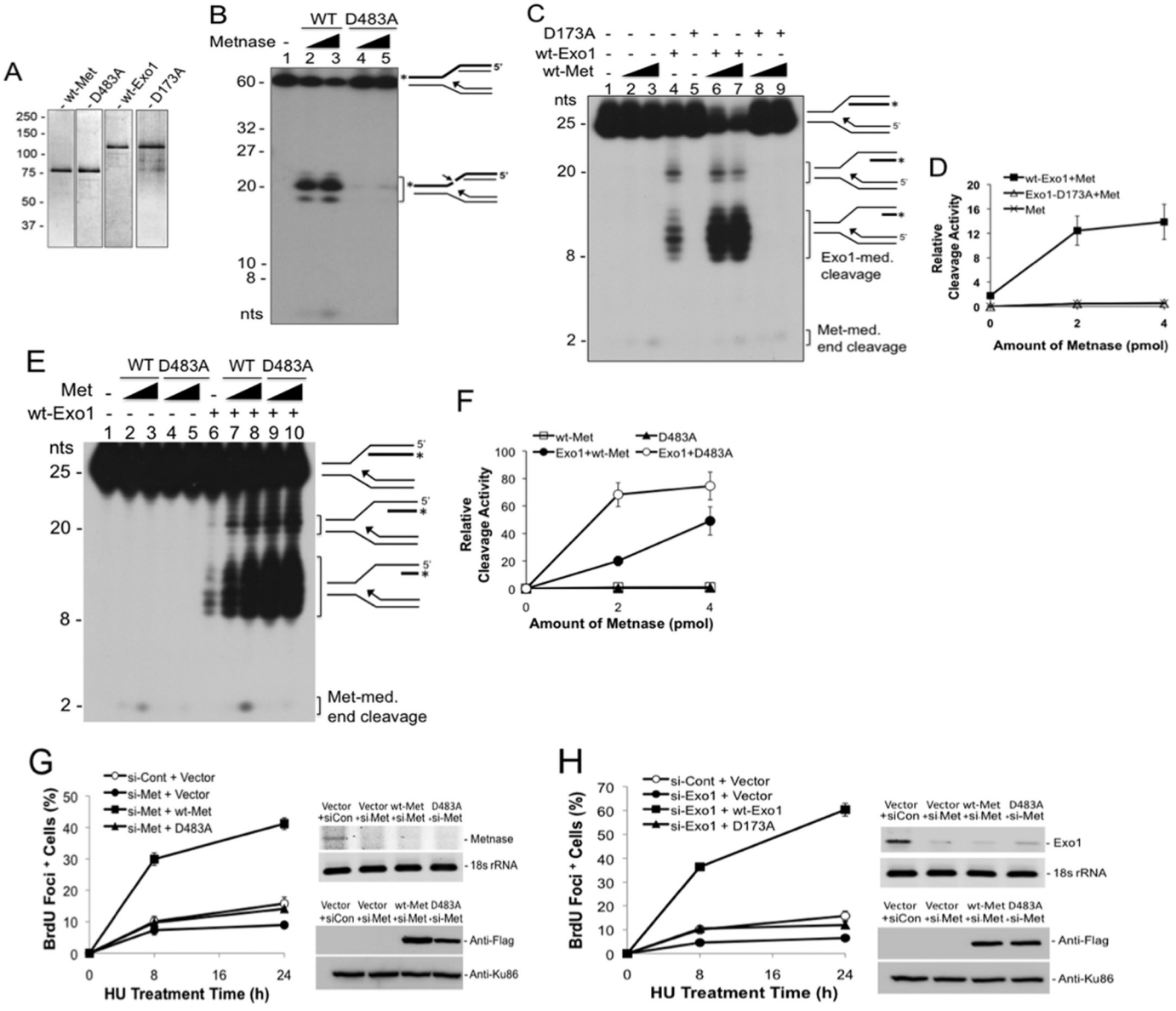

FIGURE 3. **Metnase enhances Exo1-mediated 5′-end resection of fork DNA.** *A*, silver staining of purified WT and nuclease-dead mutant of Metnase (*Met*) and Exo1 following 8% SDS-PAGE. *B*, Metnase-mediated ss-overhang cleavage with fork DNA in the presence of WT Metnase or the nuclease-dead mutant (D483A) (2 and 4 pmol). *Numbers* on the *left* indicate DNA size makers. *C* and *D*, Exo1-mediated (*med*.) 5′-end resection of the lagging daughter strand in the presence or absence of WT Metnase. D173A is a nuclease-dead mutant of Exo1. Reaction mixtures (20 μl) containing 240 fmol of 3′-^{32}P-labeled fork DNA were incubated at 37 °C in the presence of 2 mM $MgCl_2$ for 90 min, and cleavage products were analyzed by 12% PAGE containing 8 M urea. Where indicated, 2 fmol of WT or mutant Exo1 and 2–4 pmol of Metnase were used. Cleavage of 3′-^{32}P-labeled (*) lagging daughter DNA is highlighted with a *bold line* in the fork schematics on the *left*. *D*, cleavage of the lagging daughter DNA (*C*) was quantified using a PhosphorImager and ImageQuant software. Data represent average ± S.E. for three distinct determinations per condition. *Error bars* represent S.E. *E*, Metnase's DNA cleavage activity is not necessary for Exo1-mediated 5′ resection of the lagging daughter DNA. Exo1-mediated 5′-end resection of the lagging daughter strand DNA was examined in the presence of 2 and 4 pmol of either WT Metnase (*WT*) or a nuclease-dead mutant (*D483A*). Cleavage is indicated as in *C*. *F*, quantitation of lagging daughter strand cleavage in *E*. Data represent averages ± S.E. for three distinct determinations per condition. *Error bars* represent S.E. *G* and *H*, DNA cleavage activities of both Metnase and Exo1 are necessary for DNA resection at stalled replication forks. DNA resection of stalled fork was measured with anti-BrdU antibodies without denaturation of genomic DNA in HEK293 cells stably expressing WT Metnase and a nuclease-dead D483A mutant (*G*) or WT Exo1 and a nuclease-dead D173A mutant (*H*) after HU treatment. Data represent the average ± S.E. for three distinct determinations per condition. *Error bars* represent S.E. *Right*, relative expression levels of siRNA-resistant FLAG-Metnase and V5-Exo1 (wild type and the mutant). *nts*, nucleotides; *Con*, control.

tion mutation at conserved Arg residues within the HTH motif of DNA binding domain (R339A and R371A; Fig. 4*C*) not only destroyed Metnase's DNA binding activity (Fig. 4*E*) but also led to a failure in Exo1 loading onto single strand overhangs (Fig. 4*F*). A nuclease-dead mutant of Metnase (D483A), however, was effective in loading Exo1 onto DNA (Fig. 4*F*). A mutation at a key DNA binding or DNA cleavage site of Metnase has no effect on the Metnase-Exo1 interaction (Fig. 4*G*). Taken together, these results suggest that Metnase HTH and NUMOD1 DNA binding domains mediate Metnase binding to single strand overhangs and Exo1 loading onto DNA.

Enhancement of Exo1-mediated Resection by Metnase Does Not Require Metnase's DNA Cleavage Activity but Depends on the Presence of ss-Overhang DNA—Metnase's role in the loading of Exo1 onto single strand overhangs might be directly linked to enhancement of Exo1-mediated 5′ resection at fork

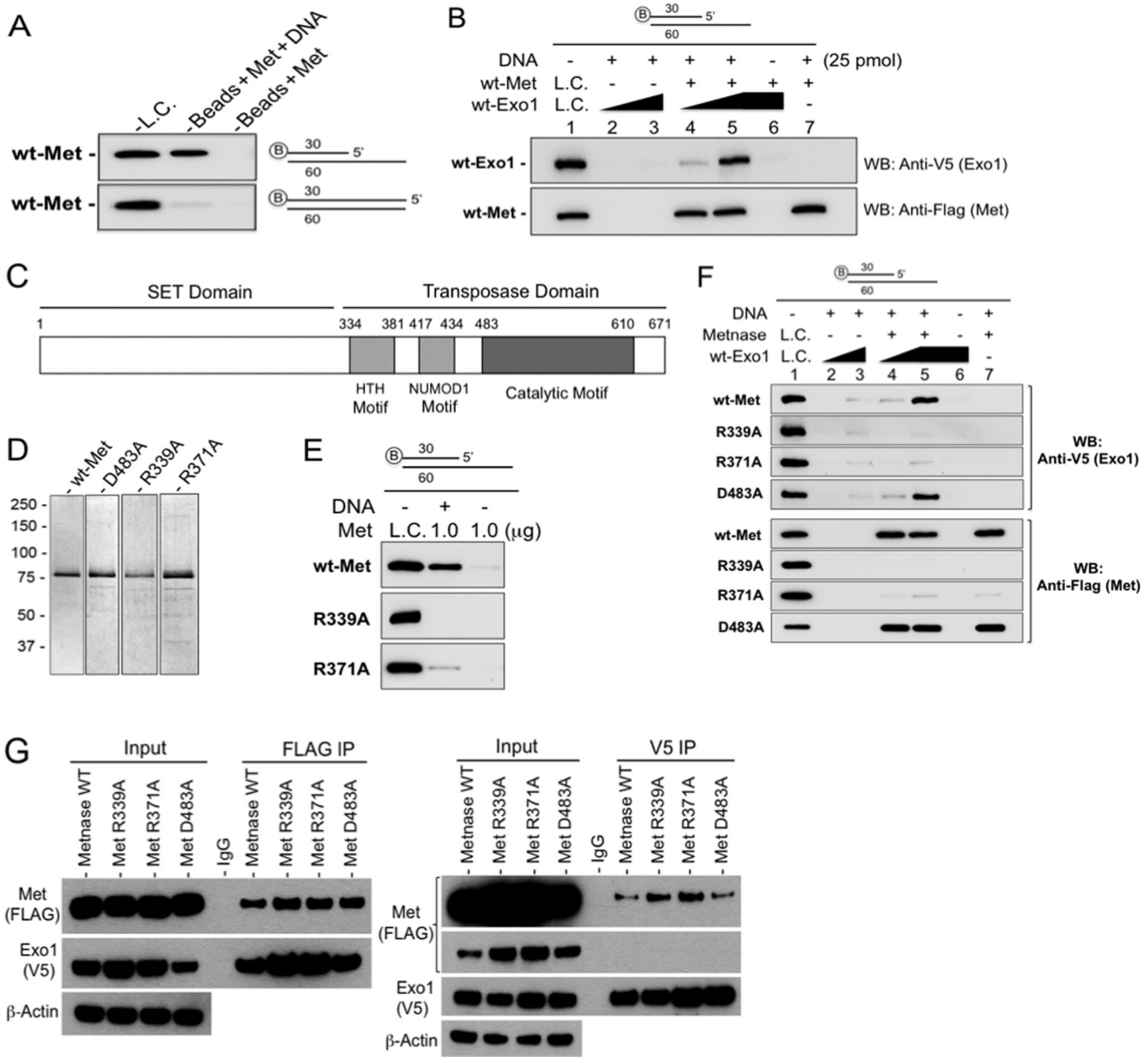

FIGURE 4. **Metnase mediates Exo1 loading onto single strand overhang DNA.** *A*, ss-overhang is required for binding of WT Metnase (*Met*) to duplex DNA. FLAG-tagged WT Metnase (1.0 μg) was incubated with 25 pmol of the 3′-biotinylated partial (*top*) or full (*bottom*) duplex DNA to assay protein-DNA binding by streptavidin-agarose beads. "*B*" indicates biotin label. The protein-DNA interaction was analyzed by Western blotting (*WB*) using an anti-FLAG antibody. *L.C.* represents the loading control of WT Metnase (0.1 μg). *B*, WT Metnase is required for Exo1 binding to a partial duplex DNA with 3′-ss-overhang in streptavidin-agarose pulldown assay. Where indicated, 1 μg of WT Metnase and two concentrations of Exo1 (0.5 and 1 μg) were used. *C*, a diagram of Metnase domains. Two DNA binding motifs (HTH and NUMOD1 motifs) and the catalytic motif reside within the transposase domain. *D*, silver staining of purified WT Metnase and the mutants following 8% SDS-PAGE. *E*, two Arg residues in the HTH motif are essential for Metnase-DNA interaction. Where indicated, 25 pmol of the 3′-biotinylated partial duplex DNA was used. *F*, Metnase mutants lacking DNA binding activity failed to mediate loading of WT Exo1 onto ss-overhang DNA. Where indicated, 1 μg of either WT or mutant Metnase and 0.5 and 1 μg of Exo1 were used. *G*, a mutation at a key DNA binding or DNA cleavage site of Metnase has no effect on the Metnase-Exo1 interaction. HEK293 cells stably expressing V5-Exo1 were transfected with WT or the mutant FLAG-Metnase and immunoprecipitated (*IP*) with FLAG (*left panel*) or V5 antibody (*right panel*), and Western blots were probed with V5, FLAG, and β-actin antibodies.

DNA. To test this, we first examined WT Exo1 for cleavage of blunt-ended dsDNA and dsDNA with ss-overhang in the presence and absence of WT Metnase. Exo1 exhibited no DNA cleavage activity with a blunt-ended dsDNA even in the presence of WT Metnase (Fig. 5*A*). A duplex DNA with single strand overhangs not only supported Exo1's 5′ resection activity (Fig. 5*B*, *lanes 2* and *3*) but also was necessary for enhancement of Exo1's resection activity by Metnase (Fig. 5, *B*, *lanes 2* and *3 versus lanes 5* and *6*, and *C*). We next examined Exo1's cleavage activity with dsDNA containing various sizes of 3′-ss-overhangs. A duplex DNA with a ≥9-nucleotide 3′-ss-overhang was able to support Exo1's 5′ resection activity that was further stimulated 5–10-fold in the presence of WT Metnase (Fig. 5, *D* and *E*), suggesting that 3′-ss-overhang is not only essential for Exo1's 5′-end resection activity but also crucial for Metnase's role in enhancing Exo1 activity. Similar to Exo1 loading onto single strand overhangs by Metnase (Fig. 4*F*), Metnase mutants defective in DNA binding (R339A and R371A) failed to enhance Exo1's end resection activity (Fig. 5, *F* and *G*), whereas

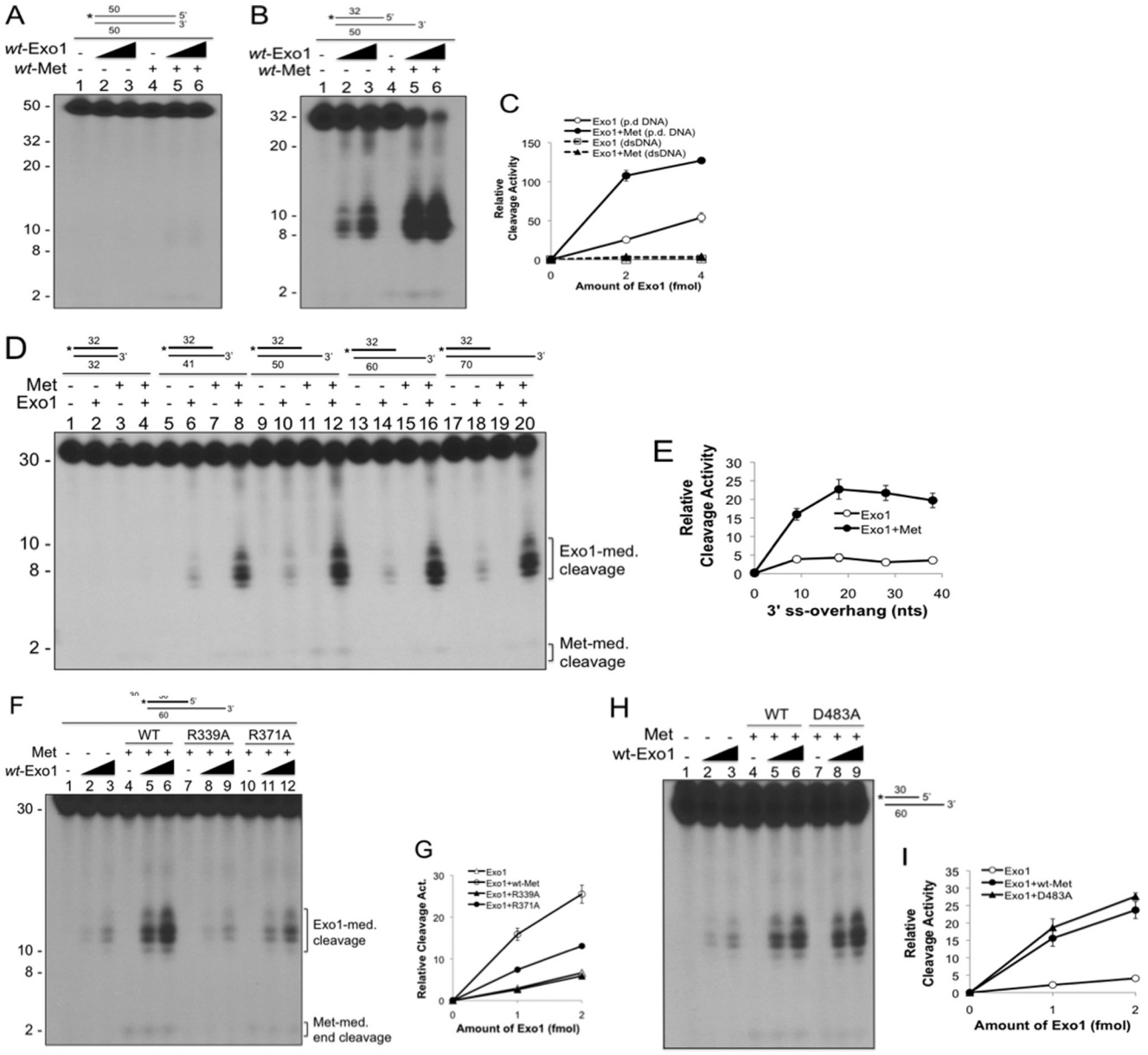

FIGURE 5. **Enhancement of Exo1's cleavage activity by Metnase depends on the presence of ss-overhang at dsDNA and Metnase's DNA binding activity.** *A* and *B*, ss-overhang is essential for Exo1-mediated DNA cleavage. The indicated amounts of WT Metnase (*Met*) and/or WT Exo1 were incubated with 240 fmol of the 3′-^{32}P-labeled duplex DNA (*A*) or the 3′-^{32}P-labeled partial duplex (*p.d.*) DNA (*B*), and cleavage products were analyzed by 12% PAGE containing 8 M urea. *C*, representative data are shown in *A* and *B*. Data represent the average ± S.E. for three distinct determinations per condition. *Error bars* represent S.E. *D*, a 9-mer of ss-overhang is enough for Metnase to enhance Exo1-mediated (*med.*) end resection activity. Reaction mixtures contained 240 fmol of 3′-^{32}P-labeled duplex DNA in different lengths of 3′-ss-overhang (bottom strand; none, *lanes 1–4*; 9-mer, *lanes 5–8*; 18-mer, *lanes 9–12*; 28-mer, *lanes 13–16*; and 38-mer, *lanes 17–20*) for 90 min prior to 12% denatured PAGE analysis. Exo1- and Metnase-mediated cleavages are marked on the *right*. *E*, Exo1-mediated 5′-end resection in the presence and absence of Metnase shown in *D* was quantified. *Error bars* represent S.E. *F*, Metnase's DNA binding activity is essential for enhancement of Exo1-mediated 5′-end resection of a partial duplex DNA. Exo1's resection activity with a partial duplex DNA was examined in the presence of either WT Metnase or a mutant defective in DNA binding activity (R339A and R371A). *G*, representative data are shown in *F*. Data represent the average ± S.E. for three distinct determinations per condition. *Error bars* represent S.E. *H*, Metnase's DNA cleavage activity (*Act.*) is not required for enhancement of Exo1's 5′-end resection activity with a partial duplex DNA. *I*, cleavage of 3′-^{32}P-labeled (*) partial duplex DNA (*H*) was quantified. Data represent the average ± S.E. for three distinct determinations per condition. *Error bars* represent S.E.

a nuclease-dead mutant (D483A) showed the same activity as WT Metnase (Fig. 5, *H* and *I*), suggesting that Metnase enhances Exo1's end resection activity by mediating Exo1 loading onto single strand overhangs.

Discussion

The mechanism of DNA replication fork restart upon stress is complex. Many components, including DNA helicases, translocases, and nucleases, are thought to play a role in this process (1, 2, 5, 6, 11, 53). How these distinct activities cooperate to orchestrate and/or facilitate fork restart is far from clear. We previously demonstrated that a SET-transposase chimeric protein called Metnase (or SETMAR) participates in fork restart after HU treatment (39–41, 54). Metnase possesses a unique DNA cleavage activity toward fork DNA (40, 55), and its catalytic motif (DDN) is necessary for Metnase's function in repli-

cation restart (40). Metnase's SET domain is also essential for recovery from DNA damage at the replication forks following HU treatment (41), although its exact role in replication restart is not clear. In this study, we showed that Metnase is involved in stalled fork processing. Metnase interacts with Exo1 and enhances Exo1's 5′-end exonuclease activity by mediating Exo1's loading onto a gapped DNA, suggesting that Metnase has multiple roles in restart of stalled replication forks.

A long HU exposure results in a stalled replication fork in DSBs that can be restarted following recombination repair (56). Recombination repair is initiated upon the formation of ssDNA 3′-overhangs through 5′-end resection. A stalled replication fork creates unique structures, especially where both branches of the fork are double-stranded (15, 16), from which it is difficult to initiate end resection with the known end resection nucleases (13, 14, 24–26). Although Mus81 and Gen1 mediate recovery from HR intermediates such as Holliday junctions, it has also been postulated that they also can nick the stalled replication fork to initiate end resection and HR repair (15, 16). Dna2 and Exo1 then resect the 5′-ends of DSBs to generate 3′-ss-overhangs, which are essential to initiate HR (26, 34, 57). Exo1 and Dna2 have been shown to process stalled replication forks (10, 58, 59) and may work together for recombination repair at stalled replication forks (43, 60). Metnase possesses endonucleolytic activity that targets ssDNA gap on fork DNA (40, 41). Our work here demonstrated that Metnase is involved in stalled fork processing (Fig. 2). Given that both WT Metnase and the mutant (D483A) were effective in enhancing Exo1 cleavage activity with a partial duplex DNA (Fig. 3, *E* and *F*), Metnase's DNA cleavage activity does not directly affect Exo1's cleavage activity. Instead, Metnase-mediated cleavage of ssDNA gap of the lagging parent DNA generates a cleavage product dissociated from fork DNA in an *in vitro* setting, which could negatively affect Exo1's resection activity of the lagging daughter DNA (Fig. 5*I*). Cells stably expressing either a Metnase mutant (D483A) or Exo1 mutant (D173A) lacking DNA cleavage activity poorly supported DNA resection after HU treatment (Fig. 3, *G* and *H*). This is in keeping with the *in vitro* observations and suggests that DNA cleavage activity of both Metnase and Exo1 are necessary for DNA resection of the lagging strand DNA at stalled forks. Exo1 plays little or no role in fork restart after a short HU exposure (Fig. 2, *G* and *H*) but plays a positive role in resection after a long HU exposure (Fig. 2, *C* and *E*). Thangavel *et al.* (10) also saw a subtle difference between the control and the Exo1 knockdown cells in restart of stalled forks, although it was much smaller than what we observed here. Although more work needs to be done, HU incubation time could be a contributing factor for the difference between the two studies. Given that Exo1 cleaves the ssDNA gap of a replication fork structure poorly because it requires a free 5′-end to begin exonucleolysis (51–54), Metnase's DNA cleavage activity likely plays an initiating role in end resection for recombination repair at stalled replication forks.

Our previous study showed that Metnase promotes resolution of γ-H2AX (41) but is not required for formation of Rad51 foci in response to HU treatment of cells for 4 h (39). In this study, however, we found that Metnase is involved in formation of Rad51 foci after a long exposure (8–24 h) to HU (Fig. 2, *I* and *J*), suggesting that Metnase's role in the loading of Exo1 not only enhances Exo1's resection activity but is also strategically beneficial for formation of Rad51 foci in recombination repair at stalled forks.

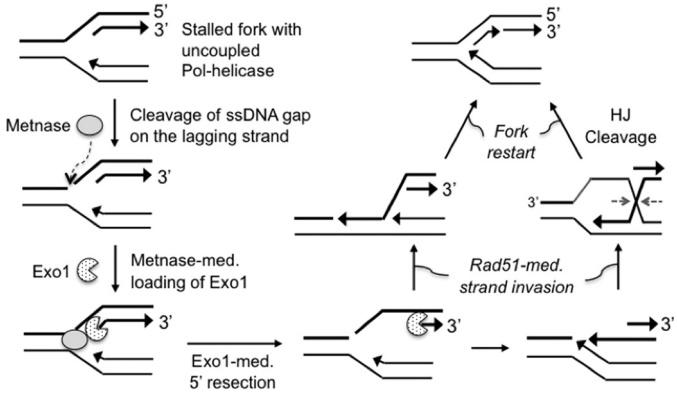

FIGURE 6. **Proposed roles of Metnase in the 5′-end resection of lagging strand during restart of stalled replication fork after HU treatment.** Lagging parental and daughter strands are highlighted with *bold lines*. *Pol*, polymerase; *HJ*, Holliday junction; *med.*, mediated.

Metnase associated with Rad9 following HU treatment (39), indicating that it works with a damage response factor(s) at the stalled forks. Metnase also interacts with topoisomerase IIα and stimulates relaxation of positive supercoils (39), which may contribute to Metnase's function in promoting fork restart. In this work, we found that Metnase interacts with Exo1, a key DNA resection factor with 5′-exonuclease activity (Fig. 1). Although the Metnase-Exo1 interaction occurs independently of HU treatment, Exo1's 5′ resection activity was significantly enhanced in the presence of Metnase (Fig. 3, *C* and *D*), suggesting that the Metnase-Exo1 interaction likely occurs on DNA. Metnase requires an ss-overhang for its binding to DNA (Fig. 4*A*) as well as for fork cleavage activity (Fig. 5, *A* and *B*). Given that Metnase's DNA binding, not DNA cleavage, activity is required for enhancement of Exo1-mediated 5′-end resection on a gapped DNA (Fig. 5, *F* and *H*), Metnase, once bound to a gapped DNA, recruits Exo1 and stabilizes the Exo1-gapped DNA interaction (Fig. 6). This Metnase-Exo1 interaction on single strand overhangs would eventually enhance Exo1's 5′-end resection activity at stalled forks. Exonuclease/endonuclease/phosphatase domain-1 (EEPD1), similar to Metnase, possesses DNA cleavage activity on a replication fork structure, interacts with Exo1, and plays a role in replication restart (59). Given that Metnase and its DNA cleavage activity play a crucial role in restart of replication (40), however, the replication fork nucleases may have a defined role for different situations.

DNA damage or replication stress causes uncoupling of DNA synthesis at replication forks and generates ssDNA gaps (62). The ssDNA gap could collapse into DSBs that are repaired by a recombination pathway (Fig. 6). Metnase knockdown sensitizes cells to HU treatment and delays restart of the replication fork (39–41, 61); its endonuclease activity (40) likely plays an initiating role in 5′-end resection by cleaving the ssDNA gap on the lagging strand template of a fork structure where both daughter branches are double-stranded flap forks prior to the stimulatory effect of Exo1 (Figs. 3*B* and 6). In the following step, Metnase interacts with Exo1 and promotes Exo1-mediated 5′-end

resection (Figs. 1 and 2), generating 3′-ssDNA for Rad51-mediated strand invasion (Fig. 6). Dna2, BLM, and the 9-1-1 clamp interact with Exo1 (25, 26, 43, 60, 63), which may also play a role in enhancing Exo1 activity. Metnase has several key characteristics that make it uniquely qualified for an initiating role in 5′-end resection on lagging strand. First, Metnase possesses endonuclease activity that preferentially cleaves a single strand gap on the lagging parent strand of fork DNA (40), whereas other end resection nucleases, such as CtIP, Exo1, and Dna2, cleave the ssDNA gap of a replication fork structure poorly because they require a free 5′-end to begin exonucleolysis (49–52). Given that Metnase interacts with Exo1 (Fig. 1) and mediates loading of Exo1 onto the ss-overhang of duplex DNA (Fig. 4), cleavage of an ssDNA gap on the lagging parent strand by Metnase would be strategically beneficial for Rad51-mediated strand transfer of the lagging template DNA at stalled replication forks (Fig. 6). Without Metnase present, HU induces far fewer single strand breaks and formation of Rad51 foci (Fig. 2*G*), consistent with that in our model of Metnase function (Fig. 6). Stalled forks that have collapsed such that they cannot be repaired often cause cell death by terminating in a DSB (2, 11, 64, 65). In this situation, DSBs from fork stalling are not an aberrant pathway leading to cell death but rather a normal step in fork repair that, when repair stalls in later steps, results in lethality.

Experimental Procedures

Chemicals, Antibodies, and DNA Substrates—[α-^{32}P]dCTP (3000 Ci/mmol) was obtained from Perkin Elmer Life Sciences and protein markers and Bradford reagents were purchased from Bio-Rad. An anti-FLAG M2 antibody was obtained from Sigma, and CldU and IdU nucleotide analogs were obtained from Sigma. Oligonucleotides were obtained from Integrated DNA Technologies (Coralville, IA).

Purification of Metnase and Exo1—WT Metnase and the mutants were purified from HEK293 cells stably expressing FLAG-tagged Metnase as described (66, 67). FLAG-Metnase was detected in cell extracts by Western blotting using a monoclonal antibody (Sigma) as described previously (66, 67). Cells overexpressing WT or mutant Metnase were suspended in 20 ml of buffer E (50 mM Tris-HCl, pH 7.5, 5 mM DTT, 1.0% Nonidet-P40, 10% glycerol, 1 mM EDTA, and mammalian protease inhibitor mixtures containing 0.2 M NaCl) and centrifuged (100,000 × *g*) for 30 min. The supernatant was filtered through a Whatman paper and incubated at 4 °C for 60 min with anti-FLAG affinity gel pre-equilibrated with buffer E. The beads were washed three times with buffer E containing 2.0 M NaCl prior to elution of the protein with buffer E containing FLAG peptide (500 μg/ml). The eluant was diluted with 10 volumes of buffer E and loaded onto a heparin-Sepharose 6 Fast Flow column (Amersham Biosciences) pre-equilibrated with buffer E. After washing the column, Metnase was fractionated using a linear gradient (0–2.0 M NaCl) in buffer E. The eluted protein was dialyzed against buffer E containing 50 mM NaCl and stored at −80 °C.

For preparation of V5-Exo1, cells were harvested; lysed with cold lysis buffer (25 mM HEPES, pH 7.5, 150 mM NaCl, 1.5 mM $MgCl_2$, 0.2 mM EDTA, 0.5% Nonidet P-40, 5 μg/ml leupeptin, 5 μg/ml antipain, 1 mM sodium orthovanadate, 1 mM NaF, 1 mM DTT, and 1 mM PMSF) for 30 min at 4 °C; and clarified by centrifugation. The cell lysates were precleared with protein G-agarose beads (Millipore) for 1 h at 4 °C with rotation, anti-V5 antibody (Invitrogen) was added and incubated overnight at 4 °C, and then protein G-agarose beads (Millipore) were added and incubated for 2 h at 4 °C. Agarose beads were collected and washed eight times with washing buffer (50 mM Tris-HCl, pH 7.5, 1.5 M NaCl, 10% glycerol, 1% Nonidet P-40, and 1 mM EDTA). Proteins were eluted with 0.2 M glycine, pH 2.5, into 1.5 M Tris-HCl, pH 8.8. The eluent was dialyzed overnight into dialysis buffer (25 mM Tris-HCl, pH 7.5, 50 mM NaCl, 20% glycerol, 1 mM EDTA, 0.05% Nonidet P-40, and 1 mM DTT) and concentrated using Amicon Ultra centrifugal filter units (Millipore).

SDS-Polyacrylamide Gel Electrophoresis (PAGE) and Western Blotting—For protein analysis, samples were subjected to 10% SDS-PAGE and stained with a silver staining kit (PlusOne Silver Staining kit, GE Healthcare). For Western blotting, proteins separated by SDS-PAGE were transferred to polyvinylidene difluoride (PVDF) membrane and probed with anti-FLAG (monoclonal mouse IgG; Sigma) followed by horseradish peroxidase-conjugated secondary antibody. Protein was visualized using the ECL system (Amersham Biosciences).

Preparation of ^{32}P-Labeled DNA Substrates—For 3′-^{32}P labeling of DNA, 40 pmol of the indicated ssDNA was incubated with 30 units of terminal transferase (Perkin Elmer Life Sciences) in the presence of [α-^{32}P]dCTP according to the manufacturer's protocol. The ^{32}P-labeled ssDNA was then annealed to non-labeled DNAs to prepare the indicated DNA substrates for the DNA cleavage assay.

DNA Cleavage Assay in Vitro—For preparation of DNA substrates used in DNA cleavage assays, oligonucleotides were mixed and annealed together for fork DNA (5′-^{32}P-labeled 5′-CTAGACTCGAGATGTCAAGCAGTCCTAACTTTGAGG-CAGAGTCCGTGACGCTCAGTATG-3′, 5′-CGATACTGA-GCGTCACGGACTCTGCCTCAAGACGGTAGTCAACGT-GTTACAGCTTGATG-3′, 5′-CATCAAGTCTGTAACACG-TTGACTACCGTC-3′, and 5′-GGACTGCTTGACATCTCG-AGTCTAG-3′), blunt-ended duplex DNA (3′-^{32}P-labeled 5′-GCAGTGGCTATCGTATAGTATTAGGTTGGTGACCCC-GTAAGGAAATTTT-3′ and 5′-AAAACTTTCCTTAC-GGGGTCACCAACCTAATACTATACGATAGCCACTGC-3′), and 3′-overhang partial duplex DNA (5′-TATTAGGTTG-GTGACCCCGTAAGGAAAGTTTT-3′ and 5′-AAAACTTT-CCTTACGGGGTCACCAACCTAATACTATACGATAGC-CACTGC-3′ or 5′-CGATACTGAGCGTCACGGACTCTGC-CTCAAGACGGTAGTCAACGTGTTACAGACTTGATG-3′ and 5′-TTGAGGCAGAGTCCGTGACGCTCAGTATCG-3′). The DNA cleavage assay was carried out using the previously described procedure with modification (40). Briefly, reaction mixtures (20 μl) containing 50 mM Tris-HCl, pH 7.5, 5 mM DTT, 5% glycerol, 2 μg of BSA, 2 mM $MgCl_2$, 0.05% Triton X-100, and 25 mM KCl were incubated with Metnase (2–4 pmol) and/or Exo1 (1–2 fmol) in the presence of 240 fmol of radiolabeled DNA. After incubation at 37 °C for the indicated amount of time, reaction mixtures were analyzed by 12% polyacrylamide gel electrophoresis containing 8 M urea for DNA

cleavage. The cleavage product was quantified using a PhosphorImager and ImageQuant software (GE Healthcare).

Protein-DNA Interaction Using DNA Pulldown Assay—3′-Biotinylated 5′-flap DNA (25 pmol) was incubated with streptavidin-agarose pretreated with BSA and rotated for 30 min at room temperature in the presence of 1.0 ml of buffer (50 mM Tris-HCl, pH 7.5, 25 mM KCl, 1.0 mM DTT, and 0.1 μg/ml BSA). After adding 1.0 μg of WT Metnase to the DNA-streptavidin-agarose, the mixtures were rotated for 30 min at room temperature and centrifuged for 5 min at 5,000 rpm. The precipitates were collected and washed once with 1.0 ml of the washing buffer (50 mM Tris-HCl, pH 7.5, and 25 mM KCl). After rotation for 5 min, the pellets were centrifuged for 5 min at 5,000 rpm at room temperature and analyzed by Western blotting.

DNA Resection in Vivo Using DNA Fiber Analysis after Single Labeling of Chromosomal Replication with IdU—DNA fiber analysis was carried out as described (10) with some modifications. Briefly, cells were grown in 6-well dishes (6×10^5/well), and 20 μM IdU was added to the growth medium and incubated for 20 min at 37 °C. After washing with fresh medium, cells were treated with 5 mM HU for 60 min or mock-treated and further incubated for the indicated times at 37 °C. HU stalls replication forks without generating additional DNA structural damage. Cells were harvested and resuspended in PBS, and ~1000 cells were transferred to a positively charged microscope slide (Superfrost/Plus, Daigger) and processed for DNA fiber analysis as described previously (40). Slides were mounted in PermaFluor aqueous, self-sealing mounting medium (Thermo Scientific), and DNA fibers were visualized using a confocal microscope (Olympus FV1000D, 63× oil immersion objective). Images were analyzed using Olympus FluoView software.

DNA Resection Analysis Using Anti-BrdU Immunofluorescence—DNA resection analysis was carried out as described (61) with slight modifications. HEK293 cells were transfected with si-control, si-Exo1, si-Metnase, or si-Exo1 + si-Metnase and seeded onto poly-D-lysine coverslips (18-mm diameter; neuVitro, catalog number GG-18-PDL) with fresh medium containing 40 μM BrdU for 36 h. After treatment with 10 mM HU for various times, cells were pre-extracted with 0.5% Triton X-100 and PBS for 5 min on ice and fixed with 4% paraformaldehyde for 20 min. The coverslips were blocked for 1 h with 1% BSA and PBS and incubated with mouse anti-BrdU antibody (1:250; BD Biosciences) overnight in a wet chamber at 4 °C. After washing four times, coverslips were incubated with secondary antibody donkey anti-mouse Alexa Fluor 488 (1:500; Invitrogen) for 1 h. After another four washes, samples were mounted in Vectashield HardSet mounting medium with DAPI (Vector Laboratories) on a microscope slide (Fisherfinest Premium Superfrost® microscope slides). The samples were analyzed using a confocal microscope (Olympus2 confocal microscope with 63× water immersion objective).

Formation of Rad51 Foci—HEK293 cells were seeded onto poly-D-lysine coverslips; transfected with control, Exo1, Metnase, or Exo1/Metnase siRNA 44 h-48 h later; and treated with 10 mM HU for various times (0, 2, 4, 8, and 24 h). Cells were pre-extracted with 0.5% Triton X-100 and PBS for 5 min on ice and fixed with 4% paraformaldehyde for 20 min. The coverslips were blocked for 1 h with 1% BSA and PBS and incubated with primary antibody rabbit polyclonal anti-Rad51 antibody (1:100; H-92, Santa Cruz Biotechnology, catalog number sc-8349) overnight in a wet chamber at 4 °C. After washing four times with PBS, coverslips were incubated with secondary antibody goat anti-rabbit Alexa Fluor 594 (1:500; Invitrogen) for 1 h. After four washes with TBS, coverslips were mounted and imaged by confocal microscopy.

Restart of Replication Forks—Two separate approaches were used to measure fork restart. The first approach is BrdU incorporation where HEK293 cells were seeded onto poly-D-lysine coverslips and transfected with control, Exo1, or Metnase siRNA. 44–48 h later, cells were treated with 10 mM HU for 18 h and then released into medium with 20 μM BrdU for 30 min. After washing, cells were fixed with ice-cold methanol/acetone, denatured with 2.0 M HCl for 30 min, and neutralized for 2 min with 0.1 M $Na_2B_4O_7$. The coverslips were blocked for 1 with 5% BSA and PBS and incubated with primary antibody mouse anti-BrdU antibody (1:250; BD Biosciences) for 1.5 h in a wet chamber at room temperature. After washing four times with 0.2% Tween 20 and PBS, coverslips were incubated with secondary antibody donkey anti-mouse Alexa Fluor 488 (1:500; Invitrogen) for 1 h. After washing four times with 0.2% Tween 20 and PBS, the samples were mounted in Vectashield HardSet mounting medium with DAPI on a microscope slide (Fisherfinest Premium Superfrost microscope slides) and analyzed using a confocal microscope (Olympus2 confocal microscope with 63× water immersion objective). In the second approach, we carried out DNA fiber analysis as described previously (40). Cells were grown in 6-well dishes (6×10^5/well), and 20 μM IdU was added to growth medium and incubated for 20 min at 37 °C. After washing with fresh medium, cells were treated with 5 mM HU for 60 min or mock-treated. Medium was replaced with fresh medium containing 100 μM CldU, and cells were further incubated for the indicated times at 37 °C. Cells were harvested and resuspended in PBS, and ~1000 cells were transferred to a positively charged microscope slide (Superfrost/Plus) and processed for DNA fiber analysis as described previously (40). Slides were mounted in PermaFluor aqueous, self-sealing mounting medium, and DNA fibers were visualized using a confocal microscope (Olympus FV1000D, 63× oil immersion objective). Images were analyzed using the Olympus FluoView software.

Statistical Analysis—All experiments were performed at least three times. Data are the means ± S.E. Statistical significance between groups was determined using analysis of variance with Tukey's post hoc test or Student's *t* test as indicated.

Author Contributions—S.-H. L. and H.-S. K. conceived the project, designed the study, and performed and analyzed all the experiments. H.-S. K., E. A. W., R. A. H., and S.-H. L. contributed reagents and materials. S.-H. L., J. A. N., R. A. H., E. A. W., and H.-S. K. analyzed the data and wrote the paper.

Acknowledgment—Imaging data were generated in the Biological Microscopy Shared Resource Facilities in the Indiana University School of Medicine.

References

1. Petermann, E., and Helleday, T. (2010) Pathways of mammalian replication fork restart. *Nat. Rev. Mol. Cell Biol.* **11,** 683–687
2. Carr, A. M., and Lambert, S. (2013) Replication stress-induced genome instability: the dark side of replication maintenance by homologous recombination. *J. Mol. Biol.* **425,** 4733–4744
3. Lambert, S., and Carr, A. M. (2013) Impediments to replication fork movement: stabilisation, reactivation and genome instability. *Chromosoma* **122,** 33–45
4. Lambert, S., and Carr, A. M. (2013) Replication stress and genome rearrangements: lessons from yeast models. *Curr. Opin. Genet. Dev.* **23,** 132–139
5. Yeeles, J. T., Poli, J., Marians, K. J., and Pasero, P. (2013) Rescuing stalled or damaged replication forks. *Cold Spring Harb. Perspect. Biol.* **5,** a012815
6. Heller, R. C., and Marians, K. J. (2006) Replisome assembly and the direct restart of stalled replication forks. *Nat. Rev. Mol. Cell Biol.* **7,** 932–943
7. Allen, C., Ashley, A. K., Hromas, R., and Nickoloff, J. A. (2011) More forks on the road to replication stress recovery. *J. Mol. Cell. Biol.* **3,** 4–12
8. Aguilera, A., and Gómez-González, B. (2008) Genome instability: a mechanistic view of its causes and consequences. *Nat. Rev. Genet.* **9,** 204–217
9. Zellweger, R., Dalcher, D., Mutreja, K., Berti, M., Schmid, J. A., Herrador, R., Vindigni, A., and Lopes, M. (2015) Rad51-mediated replication fork reversal is a global response to genotoxic treatments in human cells. *J. Cell Biol.* **208,** 563–579
10. Thangavel, S., Berti, M., Levikova, M., Pinto, C., Gomathinayagam, S., Vujanovic, M., Zellweger, R., Moore, H., Lee, E. H., Hendrickson, E. A., Cejka, P., Stewart, S., Lopes, M., and Vindigni, A. (2015) DNA2 drives processing and restart of reversed replication forks in human cells. *J. Cell Biol.* **208,** 545–562
11. Zeman, M. K., and Cimprich, K. A. (2014) Causes and consequences of replication stress. *Nat. Cell Biol.* **16,** 2–9
12. Bunting, S. F., Callén, E., Wong, N., Chen, H. T., Polato, F., Gunn, A., Bothmer, A., Feldhahn, N., Fernandez-Capetillo, O., Cao, L., Xu, X., Deng, C. X., Finkel, T., Nussenzweig, M., Stark, J. M., *et al.* (2010) 53BP1 inhibits homologous recombination in Brca1-deficient cells by blocking resection of DNA breaks. *Cell* **141,** 243–254
13. Chapman, J. R., Taylor, M. R., and Boulton, S. J. (2012) Playing the end game: DNA double-strand break repair pathway choice. *Mol. Cell* **47,** 497–510
14. Symington, L. S., and Gautier, J. (2011) Double-strand break end resection and repair pathway choice. *Annu. Rev. Genet.* **45,** 247–271
15. Rass, U. (2013) Resolving branched DNA intermediates with structure-specific nucleases during replication in eukaryotes. *Chromosoma* **122,** 499–515
16. Schwartz, E. K., and Heyer, W. D. (2011) Processing of joint molecule intermediates by structure-selective endonucleases during homologous recombination in eukaryotes. *Chromosoma* **120,** 109–127
17. Truong, L. N., Li, Y., Shi, L. Z., Hwang, P. Y., He, J., Wang, H., Razavian, N., Berns, M. W., and Wu, X. (2013) Microhomology-mediated end joining and homologous recombination share the initial end resection step to repair DNA double-strand breaks in mammalian cells. *Proc. Natl. Acad. Sci. U.S.A.* **110,** 7720–7725
18. Bouwman, P., Aly, A., Escandell, J. M., Pieterse, M., Bartkova, J., van der Gulden, H., Hiddingh, S., Thanasoula, M., Kulkarni, A., Yang, Q., Haffty, B. G., Tommiska, J., Blomqvist, C., Drapkin, R., Adams, D. J., *et al.* (2010) 53BP1 loss rescues BRCA1 deficiency and is associated with triple-negative and BRCA-mutated breast cancers. *Nat. Struct. Mol. Biol.* **17,** 688–695
19. Callen, E., Di Virgilio, M., Kruhlak, M. J., Nieto-Soler, M., Wong, N., Chen, H. T., Faryabi, R. B., Polato, F., Santos, M., Starnes, L. M., Wesemann, D. R., Lee, J. E., Tubbs, A., Sleckman, B. P., Daniel, J. A., *et al.* (2013) 53BP1 mediates productive and mutagenic DNA repair through distinct phosphoprotein interactions. *Cell* **153,** 1266–1280
20. Escribano-Díaz, C., Orthwein, A., Fradet-Turcotte, A., Xing, M., Young, J. T., Tkáč, J., Cook, M. A., Rosebrock, A. P., Munro, M., Canny, M. D., Xu, D., and Durocher, D. (2013) A cell cycle-dependent regulatory circuit composed of 53BP1-RIF1 and BRCA1-CtIP controls DNA repair pathway choice. *Mol. Cell* **49,** 872–883
21. Feng, L., Fong, K. W., Wang, J., Wang, W., and Chen, J. (2013) RIF1 counteracts BRCA1-mediated end resection during DNA repair. *J. Biol. Chem.* **288,** 11135–11143
22. Zimmermann, M., Lottersberger, F., Buonomo, S. B., Sfeir, A., and de Lange, T. (2013) 53BP1 regulates DSB repair using Rif1 to control 5′ end resection. *Science* **339,** 700–704
23. Fenech, M., Kirsch-Volders, M., Natarajan, A. T., Surralles, J., Crott, J. W., Parry, J., Norppa, H., Eastmond, D. A., Tucker, J. D., and Thomas, P. (2011) Molecular mechanisms of micronucleus, nucleoplasmic bridge and nuclear bud formation in mammalian and human cells. *Mutagenesis* **26,** 125–132
24. Kakarougkas, A., and Jeggo, P. A. (2014) DNA DSB repair pathway choice: an orchestrated handover mechanism. *Br. J. Radiol.* **87,** 20130685
25. Nimonkar, A. V., Genschel, J., Kinoshita, E., Polaczek, P., Campbell, J. L., Wyman, C., Modrich, P., and Kowalczykowski, S. C. (2011) BLM-DNA2-RPA-MRN and EXO1-BLM-RPA-MRN constitute two DNA end resection machineries for human DNA break repair. *Genes Dev.* **25,** 350–362
26. Zhu, Z., Chung, W. H., Shim, E. Y., Lee, S. E., and Ira, G. (2008) Sgs1 helicase and two nucleases Dna2 and Exo1 resect DNA double-strand break ends. *Cell* **134,** 981–994
27. Huertas, P. (2010) DNA resection in eukaryotes: deciding how to fix the break. *Nat. Struct. Mol. Biol.* **17,** 11–16
28. Ciccia, A., and Elledge, S. J. (2010) The DNA damage response: making it safe to play with knives. *Mol. Cell* **40,** 179–204
29. McVey, M., and Lee, S. E. (2008) MMEJ repair of double-strand breaks (director's cut): deleted sequences and alternative endings. *Trends Genet.* **24,** 529–538
30. (1980) DNA repair and mutagenesis in eukaryotes. Proceedings of conference held in Atlanta, Georgia, June, 1979. *Basic Life Sci.* **15,** 1–458
31. Ceccaldi, R., Rondinelli, B., and D'Andrea, A. D. (2016) Repair pathway choices and consequences at the double-strand break. *Trends Cell Biol.* **26,** 52–64
32. Garcia, V., Phelps, S. E., Gray, S., and Neale, M. J. (2011) Bidirectional resection of DNA double-strand breaks by Mre11 and Exo1. *Nature* **479,** 241–244
33. Zhou, Y., Caron, P., Legube, G., and Paull, T. T. (2014) Quantitation of DNA double-strand break resection intermediates in human cells. *Nucleic Acids Res.* **42,** e19
34. Nicolette, M. L., Lee, K., Guo, Z., Rani, M., Chow, J. M., Lee, S. E., and Paull, T. T. (2010) Mre11-Rad50-Xrs2 and Sae2 promote 5′ strand resection of DNA double-strand breaks. *Nat. Struct. Mol. Biol.* **17,** 1478–1485
35. Warmerdam, D. O., Freire, R., Kanaar, R., and Smits, V. A. (2009) Cell cycle-dependent processing of DNA lesions controls localization of Rad9 to sites of genotoxic stress. *Cell Cycle* **8,** 1765–1774
36. Tomimatsu, N., Mukherjee, B., Catherine Hardebeck, M., Ilcheva, M., Vanessa Camacho, C., Louise Harris, J., Porteus, M., Llorente, B., Khanna, K. K., and Burma, S. (2014) Phosphorylation of EXO1 by CDKs 1 and 2 regulates DNA end resection and repair pathway choice. *Nat. Commun.* **5,** 3561
37. Tomimatsu, N., Mukherjee, B., Deland, K., Kurimasa, A., Bolderson, E., Khanna, K. K., and Burma, S. (2012) Exo1 plays a major role in DNA end resection in humans and influences double-strand break repair and damage signaling decisions. *DNA Repair* **11,** 441–448
38. Niu, H., Chung, W. H., Zhu, Z., Kwon, Y., Zhao, W., Chi, P., Prakash, R., Seong, C., Liu, D., Lu, L., Ira, G., and Sung, P. (2010) Mechanism of the ATP-dependent DNA end-resection machinery from *Saccharomyces cerevisiae*. *Nature* **467,** 108–111
39. De Haro, L. P., Wray, J., Williamson, E. A., Durant, S. T., Corwin, L., Gentry, A. C., Osheroff, N., Lee, S. H., Hromas, R., and Nickoloff, J. A. (2010) Metnase promotes restart and repair of stalled and collapsed replication forks. *Nucleic Acids Res.* **38,** 5681–5691
40. Kim, H. S., Chen, Q., Kim, S. K., Nickoloff, J. A., Hromas, R., Georgiadis, M. M., and Lee, S. H. (2014) The DDN catalytic motif is required for Metnase functions in non-homologous end joining (NHEJ) repair and replication restart. *J. Biol. Chem.* **289,** 10930–10938

41. Kim, H. S., Kim, S. K., Hromas, R., and Lee, S. H. (2015) The SET domain is essential for Metnase functions in replication restart and the 5′ end of SS-overhang cleavage. *PLoS One* **10,** e0139418
42. Gravel, S., Chapman, J. R., Magill, C., and Jackson, S. P. (2008) DNA helicases Sgs1 and BLM promote DNA double-strand break resection. *Genes Dev.* **22,** 2767–2772
43. Ngo, G. H., Balakrishnan, L., Dubarry, M., Campbell, J. L., and Lydall, D. (2014) The 9-1-1 checkpoint clamp stimulates DNA resection by Dna2-Sgs1 and Exo1. *Nucleic Acids Res.* **42,** 10516–10528
44. Sartori, A. A., Lukas, C., Coates, J., Mistrik, M., Fu, S., Bartek, J., Baer, R., Lukas, J., and Jackson, S. P. (2007) Human CtIP promotes DNA end resection. *Nature* **450,** 509–514
45. El-Shemerly, M., Janscak, P., Hess, D., Jiricny, J., and Ferrari, S. (2005) Degradation of human exonuclease 1b upon DNA synthesis inhibition. *Cancer Res.* **65,** 3604–3609
46. Shao, Z., Davis, A. J., Fattah, K. R., So, S., Sun, J., Lee, K. J., Harrison, L., Yang, J., and Chen, D. J. (2012) Persistently bound Ku at DNA ends attenuates DNA end resection and homologous recombination. *DNA Repair* **11,** 310–316
47. Murti, K. G., He, D.-C., Brinkley, B. R., Scott, R., and Lee, S.-H. (1996) Dynamics of human replication protein A subunit distribution and partitioning in the cell cycle. *Exp. Cell Res.* **223,** 279–289
48. Vassin, V. M., Wold, M. S., and Borowiec, J. A. (2004) Replication protein A (RPA) phosphorylation prevents RPA association with replication centers. *Mol. Cell. Biol.* **24,** 1930–1943
49. Lee Bi, B. I., Nguyen, L. H., Barsky, D., Fernandes, M., and Wilson, D. M., 3rd. (2002) Molecular interactions of human Exo1 with DNA. *Nucleic Acids Res.* **30,** 942–949
50. Orans, J., McSweeney, E. A., Iyer, R. R., Hast, M. A., Hellinga, H. W., Modrich, P., and Beese, L. S. (2011) Structures of human exonuclease 1 DNA complexes suggest a unified mechanism for nuclease family. *Cell* **145,** 212–223
51. Stewart, J. A., Campbell, J. L., and Bambara, R. A. (2010) Dna2 is a structure-specific nuclease, with affinity for 5′-flap intermediates. *Nucleic Acids Res.* **38,** 920–930
52. Takeda, S., Nakamura, K., Taniguchi, Y., and Paull, T. T. (2007) Ctp1/CtIP and the MRN complex collaborate in the initial steps of homologous recombination. *Mol. Cell* **28,** 351–352
53. Budzowska, M., and Kanaar, R. (2009) Mechanisms of dealing with DNA damage-induced replication problems. *Cell Biochem. Biophys.* **53,** 17–31
54. Hromas, R., Williamson, E. A., Fnu, S., Lee, Y. J., Park, S. J., Beck, B. D., You, J. S., Leitao, A., Nickoloff, J. A., and Lee, S. H. (2012) Chk1 phosphorylation of Metnase enhances DNA repair but inhibits replication fork restart. *Oncogene* **31,** 4245–4254
55. Beck, B. D., Lee, S. S., Williamson, E., Hromas, R. A., and Lee, S. H. (2011) Biochemical characterization of Metnase's endonuclease activity and its role in NHEJ repair. *Biochemistry* **50,** 4360–4370
56. Petermann, E., Orta, M. L., Issaeva, N., Schultz, N., and Helleday, T. (2010) Hydroxyurea-stalled replication forks become progressively inactivated and require two different RAD51-mediated pathways for restart and repair. *Mol. Cell* **37,** 492–502
57. Mimitou, E. P., and Symington, L. S. (2008) Sae2, Exo1 and Sgs1 collaborate in DNA double-strand break processing. *Nature* **455,** 770–774
58. Cotta-Ramusino, C., Fachinetti, D., Lucca, C., Doksani, Y., Lopes, M., Sogo, J., and Foiani, M. (2005) Exo1 processes stalled replication forks and counteracts fork reversal in checkpoint-defective cells. *Mol. Cell* **17,** 153–159
59. Hu, J., Sun, L., Shen, F., Chen, Y., Hua, Y., Liu, Y., Zhang, M., Hu, Y., Wang, Q., Xu, W., Sun, F., Ji, J., Murray, J. M., Carr, A. M., and Kong, D. (2012) The intra-S phase checkpoint targets Dna2 to prevent stalled replication forks from reversing. *Cell* **149,** 1221–1232
60. Karanja, K. K., Cox, S. W., Duxin, J. P., Stewart, S. A., and Campbell, J. L. (2012) DNA2 and EXO1 in replication-coupled, homology-directed repair and in the interplay between HDR and the FA/BRCA network. *Cell Cycle* **11,** 3983–3996
61. Wu, Y., Lee, S. H., Williamson, E. A., Reinert, B. L., Cho, J. H., Xia, F., Jaiswal, A. S., Srinivasan, G., Patel, B., Brantley, A., Zhou, D., Shao, L., Pathak, R., Hauer-Jensen, M., Singh, S., *et al.* (2015) EEPD1 rescues stressed replication forks and maintains genome stability by promoting end resection and homologous recombination repair. *PLoS Genet.* **11,** e1005675
62. Lopes, M., Foiani, M., and Sogo, J. M. (2006) Multiple mechanisms control chromosome integrity after replication fork uncoupling and restart at irreparable UV lesions. *Mol. Cell* **21,** 15–27
63. Nimonkar, A. V., Ozsoy, A. Z., Genschel, J., Modrich, P., and Kowalczykowski, S. C. (2008) Human exonuclease 1 and BLM helicase interact to resect DNA and initiate DNA repair. *Proc. Natl. Acad. Sci. U.S.A.* **105,** 16906–16911
64. Arnaudeau, C., Lundin, C., and Helleday, T. (2001) DNA double-strand breaks associated with replication forks are predominantly repaired by homologous recombination involving an exchange mechanism in mammalian cells. *J. Mol. Biol.* **307,** 1235–1245
65. Costes, A., and Lambert, S. A. (2012) Homologous recombination as a replication fork escort: fork-protection and recovery. *Biomolecules* **3,** 39–71
66. Beck, B. D., Park, S. J., Lee, Y. J., Roman, Y., Hromas, R. A., and Lee, S. H. (2008) Human Pso4 is a Metnase (SETMAR)-binding partner that regulates Metnase function in DNA repair. *J. Biol. Chem.* **283,** 9023–9030
67. Roman, Y., Oshige, M., Lee, Y. J., Goodwin, K., Georgiadis, M. M., Hromas, R. A., and Lee, S. H. (2007) Biochemical characterization of a SET and transposase fusion protein, Metnase: its DNA binding and DNA cleavage activity. *Biochemistry* **46,** 11369–11376